Maximum Power Point Tracking Controller Connecting PV System to Grid

Ahmed G. Abo-Khalil[*], Dong-Choon Lee[†], Jong-Woo Choi[**] and Heung-Geun Kim[**]

[†*]Dept. of Electrical. Eng., Yeungnam University, Gyeongbuk, Korea
[**]School of Electrical Eng. and Computer Science, Kyungpook National University, Daegu, Korea

ABSTRACT

Photovoltaic (PV) generators have nonlinear V-I characteristics and maximum power points which vary with illumination level and temperature. Using a maximum power point tracker (MPPT) with an intermediate converter can increase the system efficiency by matching the PV systems to the load. This paper presents a maximum power point tracker based on fuzzy logic and a control scheme for a single-phase inverter connected to the utility grid. The fuzzy logic controller (FLC) provides an adaptive nature for system performance. Also the FLC provides excellent features such as fast response, good performance and the ability to change the fuzzy parameters to improve the control system. A single-phase AC-DC inverter is used to connect the PV system to the grid utility and local loads. While a control scheme is implemented to inject the PV output power to the utility grid at unity power factor and reduced harmonic level. The simulation results have shown the effectiveness of the proposed scheme.

Keywords: Photovoltaic, maximum power point, fuzzy logic control, harmonic cancellation

1. Introduction

Photovoltaic generation is becoming increasingly important as a renewable resource since it offers many advantages such as incurring no fuel costs, no pollution, little maintenance, and emitting no noise compared with other alternatives. The PV modules still have relatively low conversion efficiency. Therefore, the control of maximum power point tracking for the solar array is essential to a PV system.

The amount of power generated by a PV generator

depends on the operating voltage of the array. The maximum power operating point changes with insolation level and temperature. Its V-I and V-P characteristic curves specify a unique operating point at which the maximum power is generated. At the MPP, the PV system operates at its highest efficiency[1]. Therefore, the tracking control of the MPP is a complicated process. To overcome this problem, different tracking control strategies have been proposed, which are perturbation and observation P&O[2], incremental conductance[3], parasitic capacitance [4], constant voltage [5], neural network [6], and fuzzy logic control [7]. In the literatures[8], grid-connected PV inverters have been proposed, but they merely deliver real power to the utility and fixed loads. Recently, researchers have made efforts to develop parallel PV inverters which can deliver real power and reduce harmonic currents caused by nonlinear loads[9].

Generally, there are several methods which are commonly used to determine the maximum power point. With P&O algorithms, the operating voltage V is perturbed with every MPPT cycle. As soon as the MPP is reached, V oscillates around the ideal operating voltage V_{mpp}. This causes a power loss which depends on the step width of a single perturbation. If the step width is large, the MPPT algorithm will respond quickly to sudden changes in the operating conditions with increasing losses under stable or slowly changing conditions. If the step width is very small the losses under stable or slowly changing conditions is reduced, but the system can only respond very slowly to rapid changes in temperature or illumination levels. The value of the ideal step width is system-dependent and needs to be determined experimentally. Incremental conductance algorithm has an advantage over the P&O method in that it can determine when the MPPT reaches the MPP, while the output power in the P&O method oscillates around the MPP. Also, incremental conductance can track rapidly changing irradiance conditions with higher accuracy than in the P&O method.

The FLC is somewhat easy to implement because it does not require a mathematical model system. Since it gives robust performance, the dynamic performance of the controlled PV array is improved compared with that of the conductance method. This improvement includes reduction in power oscillations and fast response compared with the output conductance method.

The harmonic problem in the utility system is not unique to the photovoltaic system. Harmonic problem is more common with almost all electronic or magnetic equipment which are connected to a utility grid. This paper proposes a method to track the maximum power point using fuzzy logic control, which is efficient in cases of atmospheric change, even when conditions change suddenly and sharply. Also this paper deals with a harmonic cancellation scheme, by which the inverter can inject the power into the utility with lower harmonics.

The proposed FLC behavior depends on the membership functions, their distribution, and the rules that influence the different fuzzy variables of the system. It is important to note that there is no formal method or accurate algorithm to determine the parameters of the controller. This means that choosing fuzzy parameters to obtain an optimum operating point depends on the experience of the system designer. The quality of the inverter output current waveform shows how efficient and reliable the control scheme is.
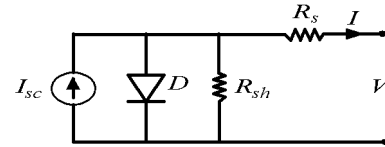

Fig. 1   Equivalent circuit of PV array

2. Mathematical Model

Solar cells are devices that convert photons into electrical potential in a PN junction, of which an equivalent circuit is shown in Fig. 1. Due to the complex physical phenomena inside the solar cell, manufacturers usually present a family of operating curves (V-I) as shown in Fig. 2. These characteristics are obtained by measuring the array volt-ampere for different illumination values. From these characteristics, the optimum voltage or current, corresponding to the maximum power point, can be determined. It is clearly seen in Fig. 2 that the current increases as the irradiance levels increases. The maximum power point increases with a steep positive slope proportional to the illumination. An increase in cell temperature results in a lower open-circuit voltage and therefore a maximum power point without significant effect in the short circuit current, as shown in Fig. 3.

The effect of cell temperature on V-I and P-V characteristics of the same array, illustrated in Fig. 2, are plotted in Fig. 3 and Fig. 4. The reduction of the maximum available PV power and the lower voltage at the peak power point are shown clearly at higher temperatures.

The main parameters which influence the illumination levels on the fixed tilt surface of the earth are the daily and seasonal solar path, the presence of clouds, mist, smog and dust between the surface and the sunlight, and the shade of the object positioned such that the illumination level is reduced, etc.

The PV output current I of PV is expressed as a function of the array voltage V

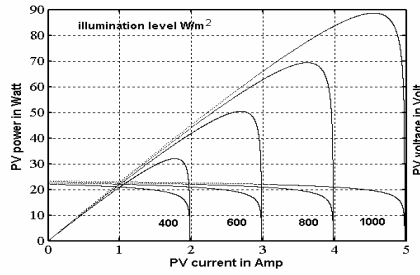$$I = I_{sc} - I_o \{e^{\frac{q(V+IR_s)}{KT_k}} - 1\} - (V + IR_s)/R_{sh} \qquad (1)$$

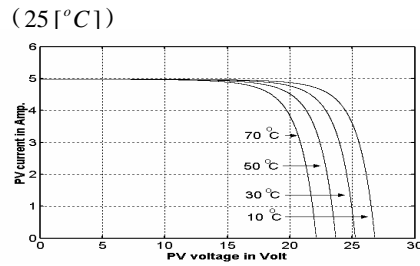Fig. 2   V-I and P-I characteristics at constant temperature

$(25[^{o}C])$

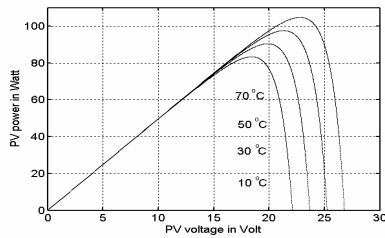Fig. 3   V-I characteristic at constant illumination (1 [kW/m^2])

Fig. 4   P-I characteristic at constant illumination (1 [kW/m^2])

where V and I represent the PV output voltage and current, respectively; R_s and R_{sh} are the series and shunt resistance of the cell (in Fig. 1); q is the electronic charge; I_{sc} is the light-generated current; I_0 is the reverse saturation current; K is the Boltzman constant, and T_k is the temperature in K.

Equation (1) can be written in another form as[2]

$$I = I_{sc}\{1 - K_1[e^{K_2 V^m} - 1]\} - (V + IR_s)/R_{sh} \qquad (2)$$

where the coefficient K_1, K_2 and m are defined as

$$K_1 = 0.01175,$$
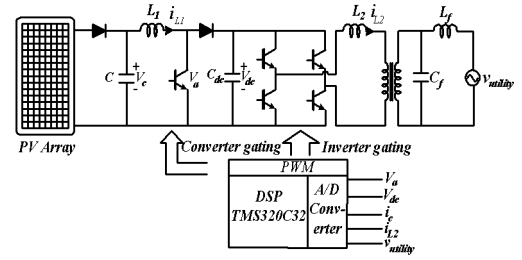$$K_2 = K_4/(V_{oc})^m,$$
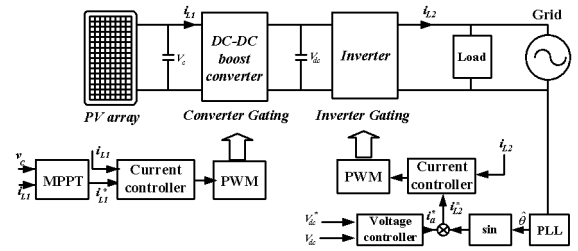$$K_4 = \ln((K_1 + 1)/K_1),$$

Fig. 5   Power circuit for PV system

Fig. 6   Control circuit for the PV system

$$K_3 = \ln[((I_{sc}(1 + K_1) - I_{mpp})/K_1 I_{sc}],$$
$$m = \ln(K_3/K_4)/\ln(V_{mpp}/V_{oc})$$

and I_{mpp} is the current at maximum output power, V_{mpp} is the voltage at maximum power, I_{sc} is the short circuit current and V_{oc} is the open circuit voltage of the array.

Equation (2) is only applicable to one particular operating condition of illumination G and cell temperature T_c. The parameter variations can be calculated by measuring the variations of the short-circuit current and the open-circuit voltage in these conditions using the parameters at normal illumination and cell temperature. Equation (2) is used for the I-V and P-V characteristics for various illuminations and fixed temperature ($25[^{o}C]$) in Fig. 2.

3. System Description

A conventional two-stage energy conversion system is connected between the PV array and the electrical power system as shown in Fig. 5. A boost converter is used to increase the PV voltage for the inverter circuit and it also plays a role in the intermediate circuit for tracking the maximum power point.

The inverter circuit converts the direct current to the

alternating current which flows into the utility or local loads. The inverter controller has two main functions. One is to synchronize the output current with the grid voltage, which means the power factor is equal to unity. The other function is to control the DC link voltage. To achieve these two goals, an inner current control loop and an outer voltage control loop are used, as shown in Fig 6.

The whole control circuit is shown in Fig. 6, the fuzzy logic controller for MPPT generates the inductor(L1) reference current which, controlled by a current controller, creates the PWM gating signal for the converter switch. Fig. 6 shows the overall control blocks for the PV generating system.

4. Control Scheme

The maximum power-matching schemes require the selected solar panel to have suitable output characteristics that can be matched with particular loads. It only approximates the location of the MPP because of its basic association with specific illumination and load conditions.

A fuzzy logic controller with linguistic control rules is adjusted to generate the maximum available system power. The structure of the fuzzy controller (number of rules, the rules themselves, number and shape of membership functions, etc.) is achieved through an essentially manual tuning process, which, although it is time-consuming, is generally faster and less problematic than corresponding procedures for conventional methods. In general, the FLC contains four main parts, two of which are the fuzzifier and defuzzifier, which perform transformations.

The other two parts are the inference engine and knowledge base. In constructing the FLC, the system input consists of the variation of the array output power, dp, and the last variation in the reference current of the boost converter, $L\delta Ic$. The output of the FLC is the new variation of the reference current of the boost converter, δI_c. The variables of dp, $L\delta Ic$, and δIc are described by triangular membership functions as shown in Fig. 7 and the control laws are given in Table I[10]. The following fuzzy levels are chosen for controlling the input and output of the FLC: n(negative), nb(negative big), nm(negative medium), ns(negative small), z(zero), p(positive), ps(positive small), pm(positive medium), and
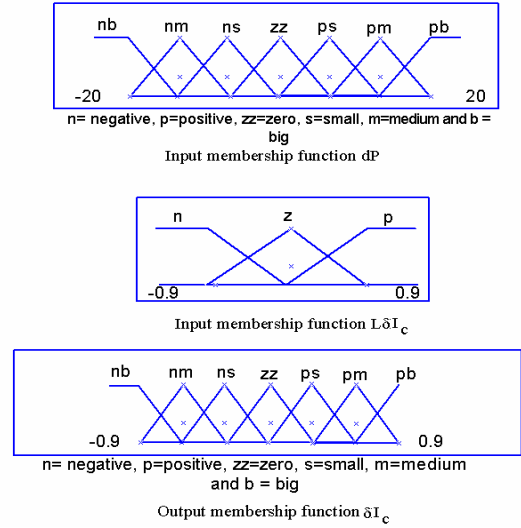
pb(positive big).

Fig. 7   Membership functions for inputs and outputs

Table 1   Rules of fuzzy logic controller

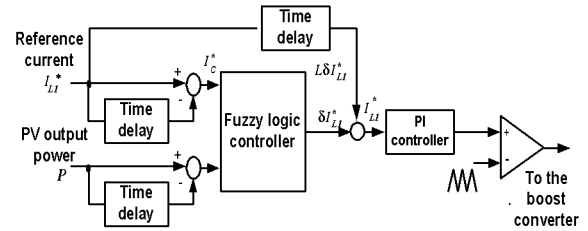|	nb	nm	ns	zz	ps	pm	pb
N	pb	pm	nm	ns	ns	nm	nb
Z	nm	ns	ns	zz	ps	ps	pm
P	nb	nm	ns	ps	ps	pm	pb

Fig. 8   Block diagram of fuzzy logic controller.

In the fuzzy logic controller, first of all, the input, $dp(k)$ and $L\delta Ic(k)$, is processed by the fuzzifier where their linguistic fuzzy subsets and fuzzy membership functions are defined. These fuzzy subsets and their fuzzy membership functions are implemented as fuzzy conditional statements. The implementation of fuzzy conditional statements results in a fuzzy subset. Its membership function, in the universe of discourse, represents control input change. This value is found by converting the fuzzy subset and its membership function into actual numbers. This conversion process is called defuzification. The input and output of the fuzzy logic

controller are shown in Fig. 8.

The output of the FLC is governed by the current controller, which modulates the reference voltage proportional to the duty ratio of the boost converter. By controlling the inductor (L1) current, the array terminal voltage is controlled to the value corresponding to the maximum power point.
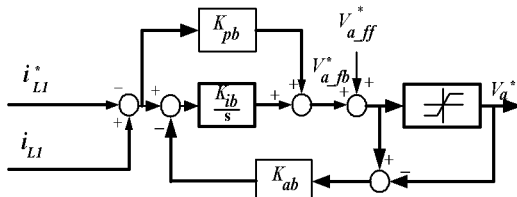

Fig. 9   Block diagram of converter current controller

In this system, changing (increasing or decreasing) the inductor current i_{L1} leads to a perturbation in the PV output power. The next direction of change can be determined by comparing the PV output power with that of the previous perturbation cycle. If the power is increasing, the next change will be made in the same direction. Fig. 9 shows the boost converter current controller, from which it can be seen v_a consists of two terms: a feedforward controller and feedback controller. The two controllers are used to obtain a fast and robust current control of i_{L1}. The reference current i_{L1}^* is the output of the FLC.

5. Harmonic Cancellation

The source of the harmonics in the inverter circuit can be classified into two categories; high frequency harmonics due to the inverter switching, and low frequency harmonics due to deficiencies in the control of inverter output current. It is difficult to cancel the low order harmonics without influencing the fundamental current waveform. For a grid-connected system, the current reference waveform of the inverter must be synchronized to the common network voltage for unity power factor. This means that the lower order harmonics coming from individual nonlinear loads are additive[7].

The grid-connected inverter has to drive the current against the supply voltage and impedance. The

performance of the grid-connected inverter was shown to be highly dependent on the grid operating conditions[13]. So it is necessary for utility-interactive systems to reduce the harmonics components in the output current at a low level.
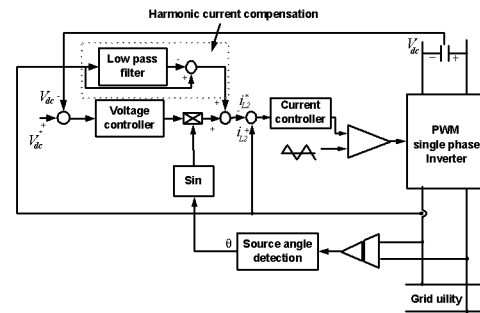

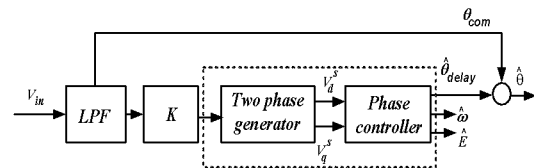Fig. 10   Control block diagram of PWM inverter

Fig. 11   Block diagram of the PLL

In this paper, the grid current controller is tuned to minimize the low order harmonics, where the conventional LC filter in the transformer primary side is replaced by the LCL filter shown in Fig. 5. The design of the LCL has already been investigated in [11]. The power rating of the converter, the line frequency and the switching frequency should be known to determine the filter parameters.

Fig. 10 shows the control block diagram including the harmonic current compensator, where the low pass filter is used for a detection of the harmonic current component. In case of capacitive loads, the change in load current can be abrupt and this change usually makes a deep notch in the grid current. A deep notch in the current produces harmonic components, which deteriorates the grid current waveform and power quality. The LCL filter and the harmonic cancellation arrangements in the transformer primary and secondary windings smoothen the grid current and reduce the harmonic contents.

Fig. 11 shows the actual PLL configuration. Since an LPF (Low Pass Filter) is inserted to reduce the noise, the gain K is multiplied to compensate for any amplitude reduction due to the LPF, while a compensation phase

(θ_{com}) is added to compensate for any phase delay due to the LPF. The transfer function for the LPF is $F(s)$, the gain K and the compensation can be expressed as

$$K = \frac{1}{\left| F(j\hat{\omega}) \right|} \tag{3}$$

$$\theta_{com} = \angle F(j\hat{\omega}) \tag{4}$$
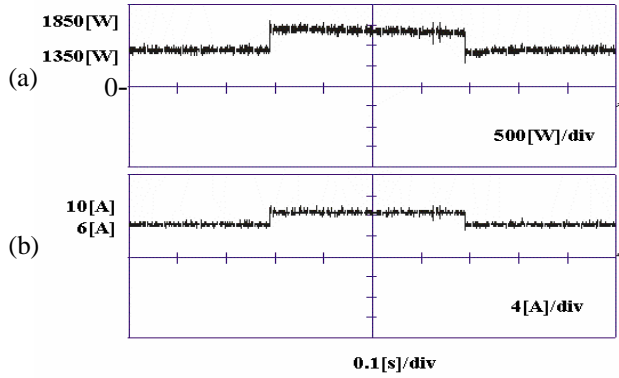

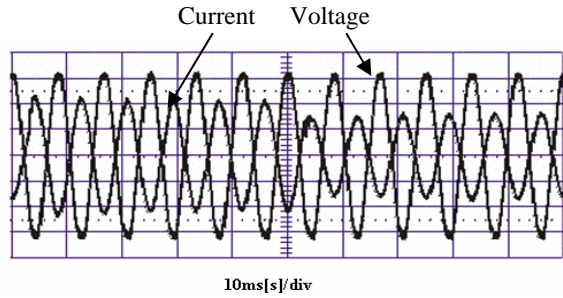Fig. 12   PV power and current at different illumination levels

Fig. 13   Instantaneous grid voltage and current waveforms

6. Experimental Results

Solar illumination varies quickly with time. It means that the maximum power point moves to another curve quickly. Such a case needs a MPPT controller capable of reaching the MPP as quickly as possible in order to reduce the output power oscillations and the system power loss. Comprehensive simulation studies were made to investigate not only the performance of the boost converter controlled by fuzzy logic algorithm but also the inverter controller performance of connecting the PV system to the grid utility at a unity power factor. The PV array was simulated using (1) and (2) as described in section II.
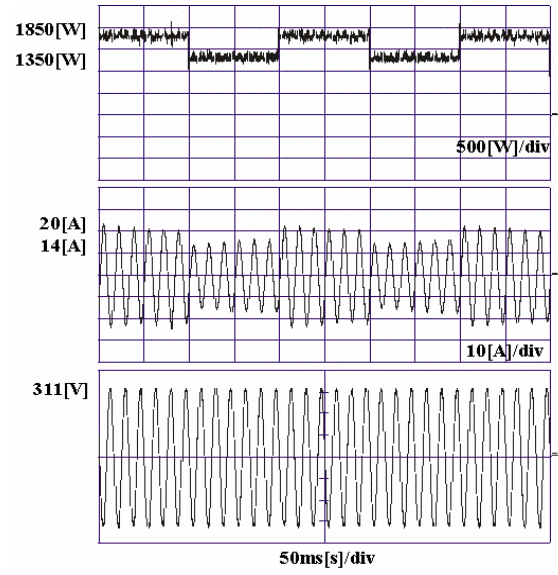

Fig. 14   Grid power, current and voltage waveform without harmonic cancellation (from top)
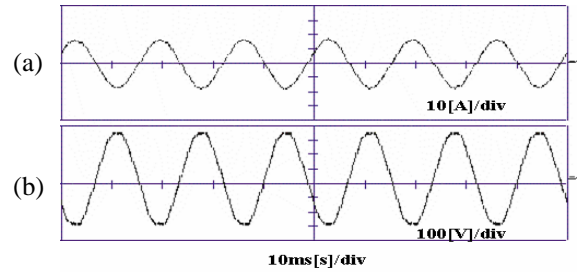

Fig. 15   Instantaneous waveforms with compensation
(a) Grid current   (b) Grid voltage

Fig. 12 shows the output power changes according to illumination variation from the starting point and also during illumination variation. The new incremental duty ratio varies according to the change in power and the last increment or decrement of the boost converter reference current. These relations between the input and output are determined in the base-rule form. It was noticed that the fast dynamic performance was obtained at step variation of illumination level.

Fig. 13 shows the unity power factor operation of the grid current and voltage. Fig. 14 shows the grid current variation with the PV power and current variation while the grid voltages remain at a sinusoidal and 220Vrms value, despite the rapid change in the illumination level and power. This indicates that the transient state response is excellent, and the conversion system provides a smooth

and stable operation. Due to this stability and smoothening, the grid current and voltage are sinusoidal as shown in Fig. 15. The simulated grid current waveform contains low order harmonics as shown in Fig. 16. A sinusoidal grid current waveform is obtained after using the harmonic cancellation algorithm as shown in Fig. 17.

The corresponding harmonic spectrum for both cases is shown in Fig. 18. Fig. 18(b) shows the harmonic spectrum of the grid current with compensation. The low order harmonic components have been suppressed almost clearly.

The performance of the harmonic cancellation technique was examined for different loads, and a noticeable improvement has been obtained. However, with
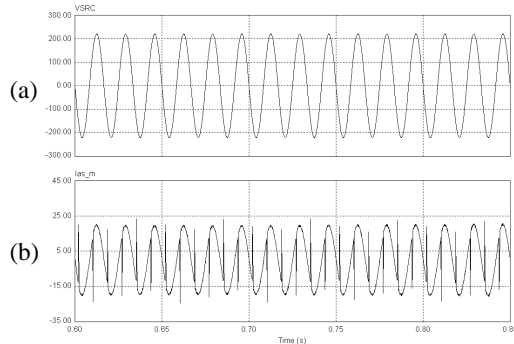
Fig. 16   Instantaneous waveforms without compensation
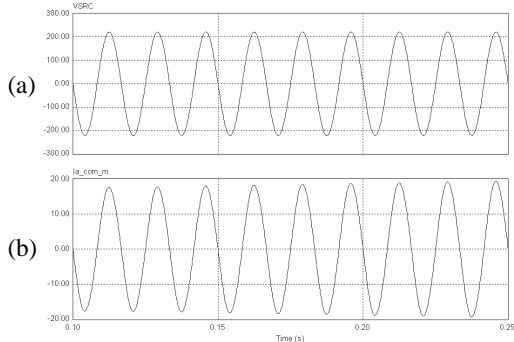(a) Grid voltage (b) Grid current

Fig. 17   Instantaneous waveforms with compensation
(a) Grid voltage (b) Grid current

the harmonic cancellation and the LCL filter arrangement, the harmonic components are reduced to nearly zero as shown in Fig. 18(b).

7. Conclusions

This paper presented a two-stage energy conversion system to connect the PV array to the grid utility and local loads. A fuzzy logic controller is used to control the boost converter in order to extract the maximum power from the PV array. It also presented an inverter control scheme to deliver the converter output power to the utility grid at unity power factor and at a reduced harmonic level. The simulation results have shown that the advantages of this system are adaptation of fuzzy parameter for fast response, good transient performance, and robustness to variations in external disturbances.
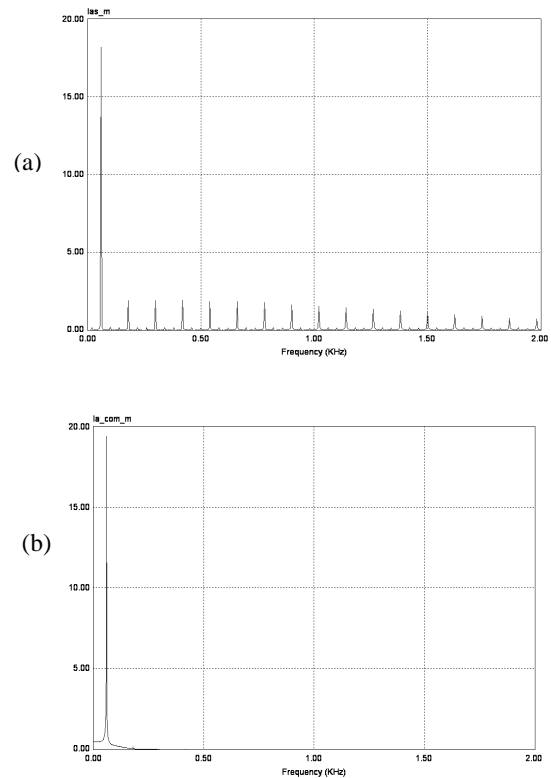
Fig. 18   Harmonic spectrum of grid current
(a) Without compensation (b) With compensation

Acknowledgment

References

[1] M. Bodur and M. Ermis, "Maximum Power Point Tracking for Low Power Photovoltaic Solar Panels," IEEE Electrotechnical Conference Proc., vol. 2, pp. 758-761, 1994.

[2] H. Sugimoto and H. Dong, "A New Scheme For Maximum Photovoltaic Power Tracking Control," IEEE Power Conversion Conference Proc., vol. 2, pp. 691-696, 1997.

[3] C. Won, "A New Maximum Power Point Tracker of Photovoltaic Arrays using Fuzzy Controller," IEEE PESC Rec., vol. 1, pp. 396–403, 1994.

[4] K. H. Hussein, I. Muta, T. Hoshino, and M. Osakada, "Maximum Photovoltaic Power Tracking: an Algorithm for Rapidly Changing Atmospheric Conditions," IEE Proc. on Generation, Transmission, and Distribution, vol. 142, no. 1, pp. 59-64, 1995.

[5] Y. Hsiao and C. Chen, "Maximum Power Tracking for Photovoltaic Power System," IEEE IAS Conf. Rec., vol. 2, pp. 1035–1040, 2002.

[6] T. Senjyu and K. Uezato, "Maximum Power Point Tracker Using Fuzzy Control for Photovoltaic Arrays," IEEE ICIT proc., pp. 143 –147, 1994.

[7] A. Al-Amoudi and L. Zhang, "Application of Radial Basis Function Networks for Solar-Array Modeling and Maximum Power-Point Prediction," IEE Proc. on Generation, Transmission and Distribution, vol. 147, no. 5, pp. 310–316, 2000.

[8] D. M. Baker, V. G. Agelidis, and C. V. Nayar, "A New Zero Average Current Error Control Algorithm for Inverter," Australian Universities Power Engineering Conference (AUPEC) proc., vol. 1, pp. 67-72, 1997.

[9] M. Armstrong, "Low Order Harmonic Cancellation Scheme for Multiple PV Grid-Connected Inverters," EPE proc., Toulouse, vol. 1, pp. 1-10, 2003.

[10] Ahmed G. Abo-Khalil, D.-C. Lee, J.-K. Seok, J.-W. Choi, and H.-G. Kim "Maximum Power Point Tracking for Photovoltaic System Using Fuzzy Logic Controller," KIPE Power Electronics Annual Conference Proc., vol. 2, pp. 503-507, 2003.

[11] M. Liserre, F. Blaabjerg, and S. Hansen, "Design and Control of an LCL-Filter-Based Three-Phase Active Rectifier," IEEE IAS Conf. Rec., vol. 1, pp. 299 - 307, 2001.

Ahmed G. Abo-Khalil was born in Egypt 1969. He received the B.Sc. and M.Sc. degrees in electrical engineering from Assiut University, Assiut, Egypt, in 1992 and 1996, respectively. He is currently working toward the Ph.D. degree at the Power Electronics and Machine Control Laboratory, Department of Electrical Engineering, Yeungnam University, Gyeongbuk, Korea. His research interests are renewable energy generation, intelligent control for electric machines and developments of power electronics circuits and systems.

Dong-Choon Lee received the B.S., M.S., and Ph.D. degrees in all electrical engineering from Seoul National University, Seoul, Korea, in 1985, 1987, and 1993, respectively. He was a Research Engineer with Daewoo Heavy Industry from 1987 to 1988. Since 1994, he has been a faculty member of the Dept. of Electrical Engineering, Yeungnam University, Gyeongbuk, Korea and currently he is a Professor. As a Visiting Scholar, he joined Power Quality Laboratory, Texas A&M University, College Station in 1998, and Electrical Drive Center, University of Nottingham, U.K. in 2001, and Wisconsin Electric Machines & Power Electronic Consortium, University of Wisconsin, Madison in 2004. His research interests include ac machine drives, control of power converters, wind power generation, and power quality.

Jong-Woo Choi was born in Taegu, Korea, in 1969. He received the B.S., M.S., and Ph.D. degrees in electrical engineering from Seoul National University, in 1991, 1993, and 1996 respectively. From 1996 to 1999, he was a Research Engineer with "LG Industrial Systems" Company. He was with "LG-OTIS Elevators" Company and "Electrical Engineering & Science Research Institute" as a Research Engineer at 2000. He was with Research Division for Information Technology, Seoul National University, as an associate professor from 2000 to 2001. Since 2001, he has been with the School of Electrical Engineering and Computer Science, Kyungpook National University, Daegu, Korea. His present research interests are in high performance electric machine control and static power conversion using power electronics.

Heung-Geun Kim was born in Korea in 1956. He received the B.S., M.S., and Ph.D. degrees in electrical engineering from Seoul National University, Seoul, Korea, in 1980, 1982, and 1988, respectively. From 1990 to 1991 he was with the Department of Electrical and Computer Engineering, University of Wisconsin, Madison, as an Honorary Fellow. Since 1984, he has been with the School of Electrical Eng. And Computer Science, Kyungpook National University, Daegu, Korea, where he is currently a Professor. His research interests are power electronic control of electric machines, electric vehicle drives, and power converter circuits.